

A Source Separation Approach to Temporal Graph Modelling for Computer Networks

Corentin Larroche

French National Cybersecurity Agency (ANSSI), Paris, France
corentin.larroche@ssi.gouv.fr

Abstract. Detecting malicious activity within an enterprise computer network can be framed as a temporal link prediction task: given a sequence of graphs representing communications between hosts over time, the goal is to predict which edges should—or should not—occur in the future. However, standard temporal link prediction algorithms are ill-suited for computer network monitoring as they do not take account of the peculiar short-term dynamics of computer network activity, which exhibits sharp seasonal variations. In order to build a better model, we propose a source separation-inspired description of computer network activity: at each time step, the observed graph is a mixture of subgraphs representing various sources of activity, and short-term dynamics result from changes in the mixing coefficients. Both qualitative and quantitative experiments demonstrate the validity of our approach.

Keywords: Cybersecurity · Anomaly detection · Temporal graphs.

1 Introduction

Besides preventive mechanisms such as firewalls and system hardening, securing computer networks requires the ability to detect ongoing intrusions in order to stop them in their tracks [25]. This need for effective intrusion detection systems has motivated the emergence of several research topics, including graph-based computer network monitoring, which represents communications between the hosts of the network as a temporal graph [19,23,27]. Intrusion detection then boils down to detecting anomalous edges in this graph. The dominant method in the literature is to reframe this problem as a temporal link prediction task, then solve this task using existing models originally designed for social network analysis [26] or content recommendation [32]. However, the short-term temporal dynamics of computer network activity differ from those of social networks and user-content interaction streams. In particular, communication patterns within an enterprise network change significantly over the course of a day and exhibit strong seasonality [31]. Therefore, models designed for social networks or recommender systems are not well suited for computer network monitoring.

To take better account of these peculiarities, we formulate the following hypothesis: at each time step, the observed activity is in fact the superposition of several activity sources (e.g., office activity, network administration, automated

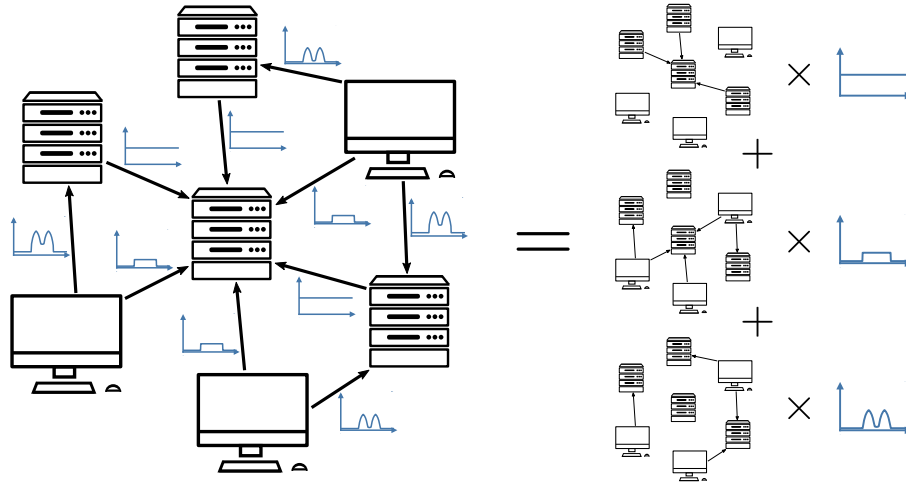


Fig. 1. The intuition behind our approach: activity within a computer network can be seen as a superposition of several activity sources, and the time-varying influence of each source is the main cause for variation in the global communication graph.

traffic), and the main cause for short-term dynamics is a change in the respective importance of each source. This setting is illustrated in Figure 1, and it provides a simple explanation for the steep, global changes observed in communication graphs over time. Following this hypothesis, modelling computer network activity can be seen as a source separation problem: given a sequence of observed graphs, we aim to learn a model for each activity source as well as the mixing coefficients for each graph. Forecasting future activity then only requires predicting a small number of mixing coefficients. In other words, such a model would have less degrees of freedom than standard temporal link predictors. The expected upside of this restrained expressivity is an increase in scalability, interpretability and robustness to noise, in turn leading to more reliable anomaly detection.

Contributions. We propose a simple model for temporal link prediction in computer networks, called Superposed Nonnegative Matrix Factorization (SNMF), of which we provide an open-source implementation¹. Qualitative and quantitative experiments demonstrate the relevance of both SNMF itself and the underlying hypothesis on the nature of the short-term dynamics of computer network activity. In particular, SNMF achieves state-of-the-art performance on a public real-world computer network monitoring dataset [17].

The rest of this paper is structured as follows. We formally define computer network monitoring and its relation to temporal link prediction, then discuss related work in Section 2. Section 3 introduces SNMF and the associated inference procedure. Our experiments are described in Section 4, and we finally discuss limitations and potential extensions of our work in Section 5.

¹ <https://github.com/cl-anssi/NetworkSourceSeparation>

2 Problem Statement and Related Work

Before describing our approach to computer network monitoring, we first provide a formal definition of this task in Section 2.1 and review previous contributions in Section 2.2.

2.1 Problem Statement — Computer Network Monitoring

Key notations. Throughout this paper, we describe communications within a computer network as a sequence of directed graphs $(\mathcal{G}_t)_{t \geq 1}$. These graphs all share the same N nodes, each of which represents one host. Each graph \mathcal{G}_t corresponds to a fixed-length time window, and there is an edge (i, j) in \mathcal{G}_t if host i has contacted host j within the t -th window. These edges are encoded as a binary adjacency matrix $\mathbf{A}_t \in \{0, 1\}^{N \times N}$. The set of all possible temporal edges is denoted $\mathcal{E} = \{(i, j, t) \in [N] \times [N] \times \mathbb{N}^* : i \neq j\}$, where $[N]$ is short for $\{1, \dots, N\}$. Note that self-loops are excluded. Finally, the element-wise product (resp. quotient) between two matrices or vectors is denoted \odot (resp. \div), the Frobenius inner product between two matrices is denoted $\langle \cdot, \cdot \rangle_{\text{F}}$, and the $N \times N$ all-one and identity matrices are called $\mathbf{1}_N$ and \mathbf{I}_N , respectively.

Problem statement. We define computer network monitoring as an anomaly ranking problem. Given a training set consisting of $T \geq 1$ graphs $(\mathcal{G}_1, \dots, \mathcal{G}_T)$ representing T successive time windows containing normal activity, our goal is to learn a link predictor $h : \mathcal{E} \rightarrow \mathbb{R}$ such that $h(i, j, t)$ is higher for normal edges than for anomalous edges. More specifically, the predictor h should minimize the false positive rate (i.e., the proportion of legitimate connections erroneously flagged as anomalous) under some detection rate constraint, meaning that edges resulting from malicious behavior should be detected with high probability.

Since traces of truly malicious behavior are hard to obtain when training and validating the model, the actual detection rate cannot be easily estimated. As a consequence, this anomaly ranking problem is usually reframed as a temporal link prediction task. In other words, the predictor h should assign higher scores to normal edges than to edges that do not occur as part of normal activity. This connection with link prediction underpins most existing work on computer network monitoring, which we further discuss in the next section.

2.2 Related Work — Temporal Graph Models

Early contributions on computer network monitoring [27,28,38] adopt a local modelling approach: each host pair (i, j) is treated independently, and its usual activity patterns are inferred based solely upon its own past activity. The main shortcoming of this approach is that it performs poorly on new edges, which have no past activity by definition. As a consequence, interest quickly shifted towards more sophisticated models designed for link prediction.

Latent space models. Despite their differences, the most popular link prediction algorithms all rely upon the following idea: each node i is associated with two dense embeddings $\mathbf{u}_i, \mathbf{v}_j \in \mathbb{R}^K$, and the presence of a link from i to j is predicted as $h(i, j) = g(\mathbf{u}_i, \mathbf{v}_j)$ for some function $g : \mathbb{R}^K \times \mathbb{R}^K \rightarrow \mathbb{R}$. This framework encompasses latent space models introduced in the social network analysis literature [12,14,15] as well as matrix factorization methods used in recommender systems [8,21,33], up to more recent link prediction techniques based on graph embedding algorithms [9,29] or graph neural networks [7,20]. We thus generically refer to all these models as latent space models. Note that some models use only one embedding per node, which boils down to setting $\mathbf{u}_i = \mathbf{v}_i$ for each node i . This is typically relevant for undirected graphs. It is also possible to include additional information such as node- or edge-related features, but we do not consider such extensions here since they are rarely used in computer network monitoring applications [1,39].

A straightforward extension of latent space models to temporal graphs consists in replacing fixed node embeddings with time series $(\mathbf{u}_{i,t}, \mathbf{v}_{i,t})_{t \geq 1}$. This leads to a temporal link predictor $h(i, j, t) = g(\mathbf{u}_{i,t}, \mathbf{v}_{j,t})$, with node embeddings typically modelled as a hidden Markov chain. Such models originated in the social network analysis [36,41] and recommender systems [10,24] communities, where they were used to model the long-term dynamics of temporal graphs. They were also recently applied to link prediction and anomaly detection in computer networks [19,23,35]. However, modelling network dynamics by adjusting node embeddings is mostly relevant for social networks and user-content interaction networks, where the evolution of the graph is smooth and driven by node-specific factors (e.g., the social environment of an individual in a social network). In contrast, activity in computer networks varies sharply (see Section 4.1 for an illustration), and short-term dynamics are mostly driven by global factors (e.g., office hours that apply to all users). As a consequence, temporal link prediction methods originally designed for social network analysis or recommender systems are not necessarily well suited for computer network monitoring.

Tensor factorization and beyond. Besides dynamic latent space models, another popular approach to temporal graph modelling relies on CANDECOMP/PARAFAC (CP) tensor factorization [3,4,13], which Eren et al. [5] proposed to use for computer network monitoring. The idea behind this approach is to represent a temporal graph as a three-mode tensor, with modes representing the time step, the origin and the destination, respectively. This leads to a link predictor $h(i, j, t) = \mathbf{w}_t \cdot (\mathbf{u}_i \odot \mathbf{v}_j)$, where $\mathbf{w}_t \in \mathbb{R}^K$ is the embedding of time step t . Interestingly, this model can be interpreted in source separation terms: each adjacency matrix \mathbf{A}_t is approximated as a linear combination of rank-one matrices

$$\hat{\mathbf{A}}_t = \sum_{k=1}^K w_{tk} \mathbf{U}_k \mathbf{V}_k^\top,$$

where \mathbf{U}_k (resp. \mathbf{V}_k) is the k -th column of the $N \times K$ embedding matrix $\mathbf{U} = (\mathbf{u}_1 \parallel \dots \parallel \mathbf{u}_N)^\top$ (resp. $\mathbf{V} = (\mathbf{v}_1 \parallel \dots \parallel \mathbf{v}_N)^\top$; \parallel denotes concatenation). Each of

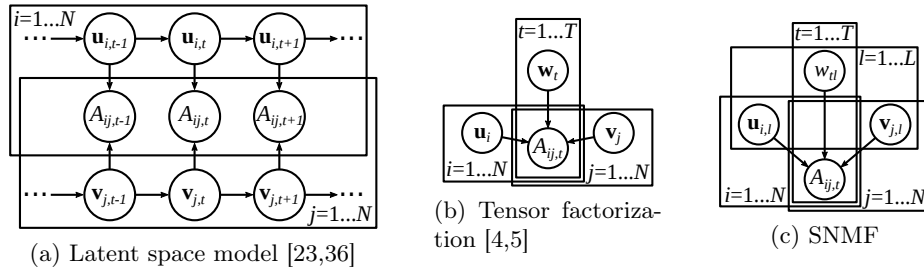


Fig. 2. Three approaches to temporal graph modelling.

these matrices can then be interpreted as an activity source, with the weights w_{t1}, \dots, w_{tK} acting as time-varying mixing coefficients. This corresponds to the setting illustrated in Figure 1, with each activity source described using a very simple model (namely, rank-one matrix factorization). Our approach, explained in the next section, builds further upon this analogy by allowing the number of activity sources to be different from (and typically smaller than) the embedding dimension K . In other words, we make the number of activity sources smaller while using a more expressive model to represent each source.

3 A Source Separation Approach to Temporal Graphs

We now move on to the description of our temporal link prediction and anomaly detection algorithm. Section 3.1 describes our model and its inference procedure, and we then address anomaly detection using the trained model in Section 3.2.

3.1 Superposed NMF — Model Description and Inference

Model description. Let $L \geq 1$ be the number of activity sources, which is treated as a hyperparameter. For each $\ell \in [L]$, we introduce origin and destination embedding matrices $\mathbf{U}_\ell, \mathbf{V}_\ell \in \mathbb{R}_+^{N \times K}$. Then, our link predictor is defined as

$$h(i, j, t) = \sum_{\ell=1}^L w_{t\ell} \mathbf{u}_{i,\ell} \cdot \mathbf{v}_{j,\ell}, \quad (1)$$

where $\mathbf{u}_{i,\ell}$ and $\mathbf{v}_{j,\ell}$ denote the i -th and j -th row of \mathbf{U}_ℓ and \mathbf{V}_ℓ , respectively. The initial mixing matrix $\mathbf{W} = (w_{t\ell}) \in \mathbb{R}_+^{T \times L}$ is learned during training, and subsequent mixing coefficients are predicted using a seasonal model (see Section 3.2).

Coming back to the source separation interpretation introduced in the previous section, Equation 1 approximates the adjacency matrix \mathbf{A}_t as a weighted sum of nonnegative matrices, each of which is modelled through nonnegative matrix factorization (NMF). We thus call this model Superposed Nonnegative Matrix Factorization (SNMF). The only time-varying parameters are the mixing coefficients w_{t1}, \dots, w_{tL} , where L is typically less than a dozen. This distinguishes

SNMF from tensor factorization, as illustrated in Figure 2: by setting the number of sources L independently from the embedding dimension K , we are able to allocate more parameters to modelling each activity source without increasing the complexity of the temporal model.

The expected benefits of a simpler model are threefold. First, it should be more robust to noise in the training data, and thus more effective for link prediction and anomaly detection. For instance, Figure 2a illustrates the structure of a dynamic latent space model (i.e., a latent space model with time-dependent node embeddings), which is much more complex and flexible than both SNMF and tensor factorization. As we show empirically in Section 4.2, this greater expressivity leads to lower link prediction and anomaly detection performance when dealing with computer network activity. Secondly, simple dynamics lead to smaller computational cost: it is indeed less expensive to predict L mixing coefficients than to adjust $2N$ node embeddings, each of size K . Finally, provided our model infers meaningful activity sources, it is more interpretable than dynamic latent space models or tensor factorizations. We demonstrate this point empirically in Section 4.1.

Model inference. Given a training sequence of adjacency matrices $(\mathbf{A}_1, \dots, \mathbf{A}_T)$, model inference boils down to finding parameters $\mathbb{U} = (\mathbf{U}_\ell)_{\ell=1}^L$, $\mathbb{V} = (\mathbf{V}_\ell)_{\ell=1}^L$, \mathbf{W} minimizing

$$J(\mathbb{U}, \mathbb{V}, \mathbf{W}) = \frac{1}{2} \sum_{t=1}^T \left\| (\mathbf{1}_N - \mathbf{I}_N) \odot \left(\mathbf{A}_t - \sum_{\ell=1}^L w_{t\ell} \mathbf{U}_\ell \mathbf{V}_\ell^\top \right) \right\|_{\text{F}}^2 + \lambda_1 \|\mathbf{W}\|_1 + \frac{\lambda_2}{2} \sum_{\ell=1}^L \left(\|\mathbf{U}_\ell\|_{\text{F}}^2 + \|\mathbf{V}_\ell\|_{\text{F}}^2 \right), \quad (2)$$

where $\lambda_1, \lambda_2 > 0$ are regularization hyperparameters and $\|\cdot\|_1$, $\|\cdot\|_{\text{F}}$ denote the L_1 and Frobenius norms, respectively. Note that we exclude the diagonal of the adjacency matrix from the computation of the mean squared error as we assume there are no self-loops. Besides, we use L_1 regularization on the mixing matrix in addition to the usual L_2 penalty on the embedding matrices. Indeed, we want to encourage sparsity in the mixing matrix as it reflects the domain-specific assumption that most activity sources are intermittent: for instance, human activity should not be observed outside office hours.

We minimize the training objective $J(\mathbb{U}, \mathbb{V}, \mathbf{W})$ using a multiplicative update procedure similar to the one proposed by Lee and Seung for standard NMF [22]. This procedure is described in Algorithm 1, and more details on its derivation can be found in Appendix A.

3.2 Anomaly Detection Using the Trained Model

Given a new temporal edge $(i, j, t) \in \mathcal{E}$ (with $t > T$), computing its anomaly score $h(i, j, t)$ as defined in Equation 1 requires knowing the weights w_{t1}, \dots, w_{tL} ,

Algorithm 1: Multiplicative update procedure for SNMF.

Data: Adjacency matrices $\mathbf{A}_1, \dots, \mathbf{A}_T$ (size $N \times N$); embedding dimension K ; number of sources L ; regularization hyperparameters λ_1, λ_2 .

Result: Mixing matrix \mathbf{W} ; embedding matrix sequences \mathbb{U} and \mathbb{V} .

Randomly initialize positive matrices $\mathbf{W}, (\mathbf{U}_1, \dots, \mathbf{U}_L), (\mathbf{V}_1, \dots, \mathbf{V}_L)$;

repeat

/* Update the mixing coefficients */

foreach $\ell \in [L], t \in [T]$ **do**

$w_{t\ell} \leftarrow w_{t\ell} \frac{\langle \mathbf{A}_t, \mathbf{U}_\ell \mathbf{V}_\ell^\top \rangle_{\mathbb{F}}}{\langle \mathbf{1}_N - \mathbf{I}_N, \mathbf{U}_\ell \mathbf{V}_\ell^\top \odot \sum_{\ell'=1}^L w_{t\ell'} \mathbf{U}_{\ell'} \mathbf{V}_{\ell'}^\top \rangle_{\mathbb{F}} + \lambda_1}$

end

/* Update the origin embedding matrices */

foreach $\ell \in [L]$ **do**

$\mathbf{M} \leftarrow \sum_{t=1}^T w_{t\ell} \left(\sum_{\ell'=1}^L w_{t\ell'} (\mathbf{1}_N - \mathbf{I}_N) \odot (\mathbf{U}_{\ell'} \mathbf{V}_{\ell'}^\top) \right) \mathbf{V}_\ell + \lambda_2 \mathbf{U}_\ell;$
 $\mathbf{U}_\ell \leftarrow \mathbf{U}_\ell \odot \left(\sum_{t=1}^T w_{t\ell} \mathbf{A}_t \mathbf{V}_\ell \right) \div \mathbf{M};$

end

/* Update the destination embedding matrices */

foreach $\ell \in [L]$ **do**

$\mathbf{M} \leftarrow \sum_{t=1}^T w_{t\ell} \left(\sum_{\ell'=1}^L w_{t\ell'} (\mathbf{1}_N - \mathbf{I}_N) \odot (\mathbf{U}_{\ell'} \mathbf{V}_{\ell'}^\top)^\top \right) \mathbf{U}_\ell + \lambda_2 \mathbf{V}_\ell;$
 $\mathbf{V}_\ell \leftarrow \mathbf{V}_\ell \odot \left(\sum_{t=1}^T w_{t\ell} \mathbf{A}_t^\top \mathbf{U}_\ell \right) \div \mathbf{M};$

end

until convergence;

return $\mathbf{W}, \mathbb{U} = (\mathbf{U}_\ell)_{\ell=1}^L, \mathbb{V} = (\mathbf{V}_\ell)_{\ell=1}^L$

which are not readily available at test time. We thus adopt a seasonal modelling approach: letting $\tau \geq 1$ denote the period of the model, we predict \mathbf{w}_t as

$$\hat{\mathbf{w}}_t = \frac{1}{|\mathcal{T}(t, \tau)|} \sum_{t' \in \mathcal{T}(t, \tau)} \mathbf{w}_{t'}, \quad \text{where } \mathcal{T}(t, \tau) = \{t' \in [t-1] : t \equiv t' \pmod{\tau}\}.$$

Typically, a reasonable value for the period τ is one week. This is the value we use in our experiments (see Section 4.2).

In addition, after fully observing and scoring a new graph \mathcal{G}_t , we learn its vector of mixing coefficients \mathbf{w}_t by minimizing the objective function of Equation 2 for the adjacency matrix \mathbf{A}_t , with \mathbb{U} and \mathbb{V} fixed. This allows the model to continuously expand its set of historical mixing coefficients, which should in turn lead to more reliable predictions using the seasonal model. Note that we have not yet implemented any forgetting mechanism, which could be useful when deploying the model for a long time (see Section 5 for further discussion of long-term dynamics and associated challenges).

Table 1. Datasets used in our experiments.

Dataset	Nodes	Time steps	Edges		
			Min.	Med.	Max.
VAST	1427	339	0	463	15,087
LANL	12,702	720	15,147	33,980.5	59,944

4 Experiments

In order to evaluate our model and test the underlying hypothesis on the nature of the short-term dynamics of computer network activity, we perform two kinds of experiments. In Section 4.1, we train SNMF on a small, well-documented dataset, which allows us to interpret and qualitatively evaluate the inferred activity sources. We then evaluate the performance of our model on link prediction and anomaly detection tasks for a larger, more complex and realistic dataset, and compare it with several state-of-the-art baselines in Section 4.2.

4.1 Qualitative Evaluation — Network Traffic Analysis

First of all, we need to assess whether our hypothesis on the dynamics of computer network activity is correct: are there such things as activity sources that can be recovered by our model? One way to answer this question is to inspect the inferred sources and mixing coefficients and confront them with our assumptions.

Dataset description. To perform this qualitative evaluation, we use a dataset that was originally generated for the Mini-Challenge 3 of the VAST 2013 competition [40]. This dataset contains two weeks of simulated network traffic involving an enterprise network and various external hosts. Note that while it contains some attacks, our main goal here is not to detect them: we only want to determine whether our model yields a meaningful decomposition of the temporal graph. Moreover, even though the synthetic nature of the data raises the question of their realism, it also provides us with a detailed knowledge of the structure of the network, the functional role of each host and the types of activity going on at any time. This allows us to confront the patterns extracted by SNMF with the ground truth.

We divide the dataset into one hour windows. For each window, we build a graph whose nodes are the hosts, identified by their IP addresses. The temporal edge (i, j, t) exists if i has initiated at least one network communication with j in time window t . See Table 1 for a description of the obtained temporal graph.

Experiment results. We train SNMF with the following hyperparameters: embedding dimension $K = 5$, number of activity sources $L = 4$, regularization coefficients $\lambda_1 = 10^{-3}$ and $\lambda_2 = 10^{-5}$. For each source ℓ , we then extract the embedding matrices $\mathbf{U}_\ell, \mathbf{V}_\ell$ and perform k -means clustering on their concatenation $(\mathbf{U}_\ell \parallel \mathbf{V}_\ell) \in \mathbb{R}_+^{N \times (2K)}$. The number of clusters is chosen by maximizing the

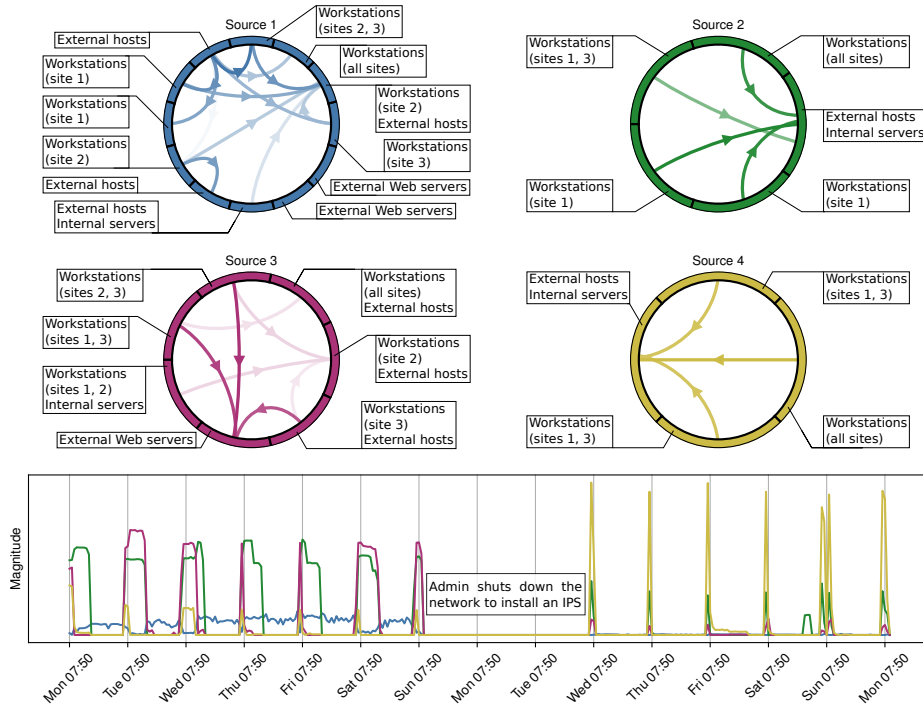


Fig. 3. Activity sources found in the VAST dataset (top) and evolution of their mixing coefficients over time (bottom). The intensity of each link reflects the total number of edges between the two clusters.

silhouette score [16]. Finally, we compute the predicted adjacency matrix $\mathbf{U}_\ell \mathbf{V}_\ell^\top$ and turn it into a graph by creating an edge (i, j) for each coefficient $\mathbf{u}_{i,\ell} \cdot \mathbf{v}_{j,\ell}$ greater than a threshold θ_ℓ . This threshold is set through manual analysis of the distribution of the coefficients.

The obtained clustered graphs are displayed along with the inferred mixing coefficients in Figure 3. The most striking observation is that the timeline can be divided into two clearly different parts, separated by a period of inactivity. This is consistent with the underlying scenario: after facing several attacks in the first week, the system administrator takes the network offline for three days in order to strengthen its defenses. In particular, an intrusion prevention system (IPS) is deployed and subsequently blocks most of the malicious traffic. These changes are clearly reflected in the mixing coefficients, which highlights the ability of SNMF to identify relevant patterns in the data. For instance, source 1, which contains inbound traffic from external hosts into the enterprise network, disappears in the second week. In contrast, sources 3 and 4, which exhibit a simple client/server structure (traffic from internal workstations to internal servers and external hosts), are dominant after the activity gap. Moreover, sources 3 and 4 exhibit a clear seasonal pattern, suggesting office-related activity, while source 1

appears to be more of a background noise partly caused by traffic coming from outside the enterprise network. Overall, Figure 3 thus demonstrates the existence of distinct activity sources that can be recovered to some extent by SNMF.

4.2 Quantitative Evaluation — Temporal Link Prediction and Anomaly Detection

We now aim to evaluate the performance of our model for temporal link prediction and malicious activity detection in computer networks. Indeed, while our primary goal is to detect edges corresponding to malicious behavior, the ability of our model to predict future edges also reflects its conformity with the true nature of the short-terms dynamics of computer network activity.

Dataset description. This quantitative evaluation is carried out using the "Comprehensive, Multi-Source Cyber-Security Events" dataset released by the Los Alamos National Laboratory [17,18]. This dataset contains event logs collected from a real-world enterprise network over 58 days. Moreover, a red team exercise took place during this time frame, meaning that security experts tried to breach the network in order to assess its security. The remote logons performed by the red team are labelled, and we thus aim to detect them. We consider the first 30 days of data and divide them into one hour windows. For each window, we build a graph whose nodes are the hosts of the enterprise network. The edge (i, j, t) exists if there is at least one remote logon from i to j in window t . See Table 1 for a description of the obtained temporal graph. We use the first seven days for training, the eighth day as a validation set and the next 22 days for evaluation.

Evaluation protocol and baselines. Besides detecting malicious logons, we also evaluate the temporal link prediction performance of SNMF. More specifically, we adopt the evaluation protocol of Poursafaei et al. [30], who propose to detect positive temporal edges among three types of negative edges:

- random negative edges, obtained by randomly rewiring positive edges;
- historical negative edges, sampled from the set of edges observed during training but not in the current time window;
- inductive negative edges, sampled from the set of edges observed in the test set but not in the training set, and not in the current time window.

For each time window t in the test set, we generate as many negative edges of each type as there are positive edges in the graph \mathcal{G}_t .

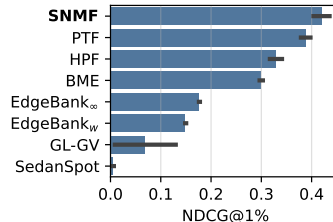
We evaluate SNMF against several baselines. First, two dynamic models are included: Poisson tensor factorization (**PTF** [5]) and the bilinear mixed-effects model proposed by Lee et al. (**BME** [23]). These two methods represent the two main approaches to dynamic latent space modelling identified in Section 2.2: adjusting all node embeddings using global time-dependent parameters, or allowing each node embedding to evolve on its own. We also include two static models: hierarchical Poisson factorization (**HPF** [35]) and the **GL-GV** model

Table 2. Mean and standard deviation of the area under the ROC curve for each task.

Method	Anomaly	Random	Historical	Inductive
SNMF	99.1±0.1	98.4±0.0	76.9±0.2	98.2±0.1
PTF [5]	97.6±0.9	98.6±0.0	68.5±0.2	96.7±0.3
BME [23]	90.3±0.2	98.5±0.0	73.3±0.0	96.2±0.0
HPF [35]	97.7±0.3	99.1±0.0	69.6±0.1	97.5±0.0
GL-GV [1]	87.0±2.4	95.8±1.0	61.2±0.5	74.6±1.9
SEDANSPOT [6]	63.6±7.3	51.2±2.2	54.7±1.4	53.2±2.7
EDGE BANK _∞ [30]	96.2±0.0	97.2±0.0	56.0±0.0	98.3±0.0
EDGE BANK _w [30]	96.0±0.0	97.0±0.0	58.0±0.0	98.1±0.0

introduced by Bowman et al. [1], which relies on the node2vec graph embedding algorithm [9]. Next up, **SEDANSPOT** [6] is a generic anomaly detection algorithm for temporal graphs: unlike other baselines, it was not specifically proposed as a computer network monitoring method. Finally, the two naive temporal link prediction methods introduced by Poursafaei et al. [30] are also evaluated: **EDGE BANK_∞** memorizes all edges seen so far and considers them normal, while its variant **EDGE BANK_w** only memorizes edges seen in the recent past. The length of the memorized window for **EDGE BANK_w** is set to one week in our experiments. As for latent space models, their hyperparameters are set by maximizing the average area under the ROC curve (AUC) for the three link prediction tasks on the validation set. In particular, the embedding dimension K is selected from the set $\{10, 20, 30, 40, 50\}$. For SNMF, the number of sources L can take the values 2, 3, 4 or 5, and the embedding dimension for each source is set to $\lfloor K/L \rfloor$ for fair comparison with the baselines.

Evaluation results. Table 2 reports the mean and standard deviation over 10 runs of the AUC for each task and each evaluated method. First of all, SNMF outperforms all baselines on the anomaly detection task, which is especially important as the main goal of our work is to detect malicious activity. Note, however, that the highly imbalanced nature of the anomaly detection task makes the AUC insufficient as an evaluation metric. Indeed, in a real-world computer network monitoring setting, only an extremely low false positive rate would be acceptable, whereas the AUC is computed on the whole ROC curve. We thus also compute the normalized discounted cumulative gain for the top 1% of the anomaly ranking (NDCG@1%), which accounts for the greater importance of the highest-

**Fig. 4.** Mean and standard deviation of the NDCG@1% score (anomaly detection task).

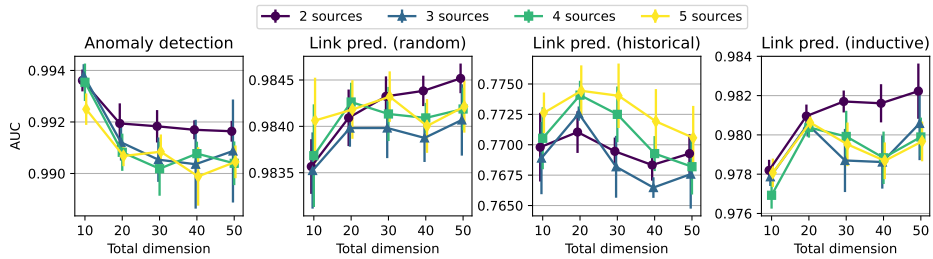


Fig. 5. Mean and standard deviation of the area under the ROC curve for each task, as a function of the number of sources L and the total dimension $L \cdot K$.

ranking temporal edges. The results, displayed in Figure 4, confirm that SNMF outperforms all baselines.

Regarding link prediction tasks, SNMF performs best on historical negative edges, which also sustains our initial hypothesis on short-term dynamics of computer network activity. Indeed, distinguishing positive edges from historical negatives requires not only memorizing edges seen during training, but also accurately modelling the corresponding temporal patterns. In particular, the fact that SNMF outperforms PTF confirms that a small number $L < K$ of activity sources is sufficient to model these patterns. As for inductive negative edges, while SNMF is the best-performing latent space model, none of these models actually outperforms the naive baseline $\text{EDGE BANK}_{\infty}$. The most likely cause for this is that new edges observed at test time in the LANL dataset are noisy events that do not reoccur frequently. As a consequence, distinguishing them from positive edges is easy, and modelling temporal patterns does not bring any improvement. A similar phenomenon occurs for random negatives, which explains why static matrix factorization performs best on this task.

Sensitivity analysis. Finally, in order to study the respective influence of the embedding dimension K and the number of sources L on the accuracy of SNMF for each task, we display the AUC as a function of L and K in Figure 5. The obtained plot for the anomaly detection task is noteworthy: increasing K degrades performance, and this decrease gets steeper as L increases. In other words, simpler models perform better, which results from the somewhat overt nature of malicious activity in the LANL dataset: the anomalous logons correspond to edges that are never observed as part of normal activity, which makes them easy to detect even without a deep understanding of the temporal dynamics. However, such knowledge would be useful for detecting stealthier attacks.

As for link prediction, increasing L up to 4 improves performance in the historical setting, but this improvement then plateaus for $L = 5$. This confirms that a few activity sources are enough, thereby demonstrating the relevance of our approach. Finally, in the random and inductive settings, simply memorizing frequently reoccurring edges leads to satisfactory performance, which explains why increasing K improves the AUC while increasing L slightly degrades it.

5 Discussion and Future Work

We now discuss limitations and potential extensions of our work, identifying several leads for future research.

Extension to more complex data and models. One important characteristic of computer network monitoring is that it produces rich and complex data. While we focus on communications between hosts and their temporal component, one important avenue of research deals with jointly modelling the many other facets of these communications, such as the associated user accounts or network protocols [5]. Note, however, that the core of our approach could easily be extended in this direction: typically, instead of predicting temporal edges (i, j, t) , we could predict hyperedges (v_1, \dots, v_d, t) using the same source separation approach, provided that the model for each activity source is adapted to such data.

In addition, we represent network activity as a sequence of graphs, each of which stands for a given time window. However, this temporal aggregation step leads to some information loss, and it could thus be interesting to directly model individual interactions between hosts instead. The stream of interactions could for instance be modelled as a marked point process, in a way similar to previous contributions on recommender systems [37] and computer network monitoring [34]. The source separation approach would then consist in modelling the stochastic intensity of this point process as a time-dependent linear combination of simpler functions representing the activity sources.

Better prediction of the mixing coefficients. As described in Section 3.2, we use a simple seasonal model to predict the vector of mixing coefficients \mathbf{w}_t at test time. However, more flexible and sophisticated methods could also be designed. For instance, an autoregressive model could be used to learn the temporal dynamics of \mathbf{w}_t . More generally, the sequence $(\mathbf{w}_t)_{t \geq 1}$ can be seen as a low-dimensional multivariate time series, and any time series forecasting method can thus be used to predict the mixing coefficients. Another possible approach, similar to the work of Gutflaish et al. [11], is to learn to predict \mathbf{w}_t based on some explicit features of the current time step (e.g. hour of day, day of week, number of observed events).

Combining short- and long-term dynamics. Finally, we emphasize that our model only addresses short-term dynamics, i.e., variations in the observed activity within a given day or week. However, computer networks are also prone to long-term dynamics, which are driven by two main causes. First, existing nodes can change their behavior: for instance, a server can start hosting a new application, thus receiving more traffic from other hosts. Secondly, the node set can evolve over time as new hosts are added to the network. These two problems are well-known in the recommender systems literature, where they are typically referred to as concept drift and cold start, respectively. While concept drift can be mitigated by partially retraining the model on a regular basis [10], addressing the cold start problem typically involves initializing a new node’s embedding based on those of old nodes whose behavior is similar [11]. Both of these procedures could easily be applied to our model.

6 Conclusion

We propose a simple model for the short-term dynamics of communications within a computer network. This model builds upon the idea that the observed activity results from the superposition of a small number of activity sources, and that short-term dynamics are mainly caused by the temporal variation of the respective weights of these sources. Both qualitative and quantitative evaluation support this hypothesis. In particular, our model outperforms state-of-the-art baselines at detecting anomalous edges resulting from malicious behavior.

These results lead to the following insights. First, computer network activity exhibits specific temporal dynamics, which differ significantly from those observed in social networks or user-content interaction streams. As a consequence, temporal link prediction models designed for such data should not be applied directly to computer networks. Secondly, these dynamics, despite their peculiarity, appear to be reasonably simple and predictable. Building upon simple models might thus be the best way forward.

A Derivation of the Inference Procedure

Training the SNMF model requires minimizing the function J defined in Equation 2, which amounts to a minimization problem subject to nonnegativity constraints. The Karush-Kuhn-Tucker (KKT) conditions [2] translate to

$$\begin{cases} \frac{\partial J}{\partial w_{t\ell}} \geq 0 & \text{and } w_{t\ell} \frac{\partial J}{\partial w_{t\ell}} = 0 & \text{for all } t \in [T], \ell \in [L] \\ \frac{\partial J}{\partial u_{ik,\ell}} \geq 0 & \text{and } u_{ik,\ell} \frac{\partial J}{\partial u_{ik,\ell}} = 0 & \text{for all } i \in [N], k \in [K], \ell \in [L] \\ \frac{\partial J}{\partial v_{jk,\ell}} \geq 0 & \text{and } v_{jk,\ell} \frac{\partial J}{\partial v_{jk,\ell}} = 0 & \text{for all } j \in [N], k \in [K], \ell \in [L] \end{cases} \quad (3)$$

where $u_{ik,\ell}$ (resp. $v_{jk,\ell}$) is the coefficient of \mathbf{U}_ℓ (resp. \mathbf{V}_ℓ) at position (i, k) (resp. (j, k)). The partial derivatives are

$$\begin{cases} \frac{\partial J}{\partial w_{t\ell}} = -\sum_{1 \leq i \neq j \leq N} \mathbf{u}_{i,\ell} \cdot \mathbf{v}_{j,\ell} \left(A_{ij,t} - \sum_{\ell'=1}^L w_{t\ell'} \mathbf{u}_{i,\ell'} \cdot \mathbf{v}_{j,\ell'} \right) + \lambda_1 \\ \frac{\partial J}{\partial u_{ik,\ell}} = -\sum_{t=1}^T \sum_{j \neq i} w_{t\ell} v_{jk,\ell} \left(A_{ij,t} - \sum_{\ell'=1}^L w_{t\ell'} \mathbf{u}_{i,\ell'} \cdot \mathbf{v}_{j,\ell'} \right) + \lambda_2 u_{ik,\ell} \\ \frac{\partial J}{\partial v_{jk,\ell}} = -\sum_{t=1}^T \sum_{i \neq j} w_{t\ell} u_{ik,\ell} \left(A_{ij,t} - \sum_{\ell'=1}^L w_{t\ell'} \mathbf{u}_{i,\ell'} \cdot \mathbf{v}_{j,\ell'} \right) + \lambda_2 v_{jk,\ell} \end{cases} \quad (4)$$

Plugging Equation 4 into the equality conditions of Equation 3 then yields

$$\begin{cases} w_{t\ell} \sum_{1 \leq i \neq j \leq N} A_{ij,t} \mathbf{u}_{i,\ell} \cdot \mathbf{v}_{j,\ell} = w_{t\ell} \sum_{1 \leq i \neq j \leq N} \sum_{\ell'=1}^L w_{t\ell'} \mathbf{u}_{i,\ell'} \cdot \mathbf{v}_{j,\ell'} + \lambda_1 \\ u_{ik,\ell} \sum_{t=1}^T w_{t\ell} \sum_{j \neq i} A_{ij,t} v_{jk,\ell} = u_{ik,\ell} \left(\sum_{t=1}^T w_{t\ell} \sum_{j \neq i} v_{jk,\ell} \sum_{\ell'=1}^L w_{t\ell'} \mathbf{u}_{i,\ell'} \cdot \mathbf{v}_{j,\ell'} \right. \\ \quad \left. + \lambda_2 u_{ik,\ell} \right) \\ v_{jk,\ell} \sum_{t=1}^T w_{t\ell} \sum_{i \neq j} A_{ij,t} u_{ik,\ell} = v_{jk,\ell} \left(\sum_{t=1}^T w_{t\ell} \sum_{i \neq j} u_{ik,\ell} \sum_{\ell'=1}^L w_{t\ell'} \mathbf{u}_{i,\ell'} \cdot \mathbf{v}_{j,\ell'} \right. \\ \quad \left. + \lambda_2 v_{jk,\ell} \right) \end{cases}$$

which leads to the multiplicative updates of Algorithm 1.

References

1. Bowman, B., Laprade, C., Ji, Y., Huang, H.H.: Detecting lateral movement in enterprise computer networks with unsupervised graph AI. In: RAID (2020)
2. Boyd, S., Vandenberghe, L.: Convex optimization. Cambridge University Press (2004)
3. Carroll, J.D., Chang, J.J.: Analysis of individual differences in multidimensional scaling via an n-way generalization of "Eckart-Young" decomposition. *Psychometrika* **35**(3), 283–319 (1970)
4. Dunlavy, D.M., Kolda, T.G., Acar, E.: Temporal link prediction using matrix and tensor factorizations. *ACM Trans. Knowl. Discov. Data* **5**(2), 1–27 (2011)
5. Eren, M.E., Moore, J.S., Alexandro, B.S.: Multi-dimensional anomalous entity detection via Poisson tensor factorization. In: ISI (2020)
6. Eswaran, D., Faloutsos, C.: Sedanspot: Detecting anomalies in edge streams. In: ICDM (2018)
7. Gilmer, J., Schoenholz, S.S., Riley, P.F., Vinyals, O., Dahl, G.E.: Neural message passing for quantum chemistry. In: ICML (2017)
8. Gopalan, P., Hofman, J.M., Blei, D.M.: Scalable recommendation with hierarchical poisson factorization. In: UAI (2015)
9. Grover, A., Leskovec, J.: node2vec: Scalable feature learning for networks. In: KDD (2016)
10. Gultekin, S., Paisley, J.: A collaborative Kalman filter for time-evolving dyadic processes. In: ICDM (2014)
11. Gutflaish, E., Kontorovich, A., Sabato, S., Biller, O., Sofer, O.: Temporal anomaly detection: calibrating the surprise. In: AAAI (2019)
12. Handcock, M.S., Raftery, A.E., Tantrum, J.M.: Model-based clustering for social networks. *J. R. Stat. Soc. A Stat.* **170**(2), 301–354 (2007)
13. Harshman, R.A.: Foundations of the PARAFAC procedure: Models and conditions for an "explanatory" multimodal factor analysis. *UCLA Work. Pap. Phon.* **16**, 1–84 (1970)
14. Hoff, P.D.: Bilinear mixed-effects models for dyadic data. *J. Am. Stat. Assoc.* **100**(469), 286–295 (2005)
15. Hoff, P.D., Raftery, A.E., Handcock, M.S.: Latent space approaches to social network analysis. *J. Am. Stat. Assoc.* **97**(460), 1090–1098 (2002)
16. Kaufman, L., Rousseeuw, P.J.: Finding groups in data: an introduction to cluster analysis. Wiley (2009)
17. Kent, A.D.: Comprehensive, multi-source cyber-security events. Los Alamos National Laboratory (2015). <https://doi.org/10.17021/1179829>
18. Kent, A.D.: Cybersecurity data sources for dynamic network research. In: *Dynamic Networks in Cybersecurity*. Imperial College Press (2015)
19. King, I.J., Huang, H.H.: EULER: Detecting network lateral movement via scalable temporal link prediction. In: NDSS (2022)
20. Kipf, T.N., Welling, M.: Variational graph auto-encoders. arXiv preprint arXiv:1611.07308 (2016)
21. Koren, Y., Bell, R.M., Volinsky, C.: Matrix factorization techniques for recommender systems. *Computer* **42**(8), 30–37 (2009)
22. Lee, D.D., Seung, H.S.: Algorithms for non-negative matrix factorization. In: *NeurIPS* (2000)
23. Lee, W., McCormick, T.H., Neil, J., Sodja, C., Cui, Y.: Anomaly detection in large-scale networks with latent space models. *Technometrics* **64**(2), 241–252 (2022)

24. Lu, Z., Agarwal, D., Dhillon, I.S.: A spatio-temporal approach to collaborative filtering. In: RecSys (2009)
25. Marchette, D.J.: Computer intrusion detection and network monitoring: a statistical viewpoint. Springer (2001)
26. Marjan, M., Zaki, N., Mohamed, E.A.: Link prediction in dynamic social networks: A literature review. In: CIST (2018)
27. Neil, J., Hash, C., Brugh, A., Fisk, M., Storlie, C.B.: Scan statistics for the online detection of locally anomalous subgraphs. *Technometrics* **55**(4), 403–414 (2013)
28. Neil, J., Uphoff, B., Hash, C., Storlie, C.: Towards improved detection of attackers in computer networks: New edges, fast updating, and host agents. In: ISRCS (2013)
29. Perozzi, B., Al-Rfou, R., Skiena, S.: Deepwalk: Online learning of social representations. In: KDD (2014)
30. Poursafaei, F., Huang, S., Pelrine, K., Rabbany, R.: Towards better evaluation for dynamic link prediction. In: NeurIPS (2022)
31. Price-Williams, M., Turcotte, M.J., Heard, N.: Time of day anomaly detection. In: EISIC (2018)
32. Rabiu, I., Salim, N., Da’u, A., Osman, A.: Recommender system based on temporal models: a systematic review. *Appl. Sci.* **10**(7), 2204 (2020)
33. Salakhutdinov, R., Mnih, A.: Probabilistic matrix factorization. In: NeurIPS (2007)
34. Sanna Passino, F., Heard, N.A.: Mutually exciting point process graphs for modeling dynamic networks. *J. Comput. Graph. Stat.* pp. 1–15 (2022)
35. Sanna Passino, F., Turcotte, M.J., Heard, N.A.: Graph link prediction in computer networks using Poisson matrix factorisation. *Ann. Appl. Stat.* **16**(3), 1313–1332 (2022)
36. Sarkar, P., Moore, A.W.: Dynamic social network analysis using latent space models. In: NeurIPS (2005)
37. Shang, J., Sun, M.: Local low-rank Hawkes processes for temporal user-item interactions. In: ICDM (2018)
38. Turcotte, M., Heard, N., Neil, J.: Detecting localised anomalous behaviour in a computer network. In: IDA (2014)
39. Turcotte, M., Moore, J., Heard, N., McPhall, A.: Poisson factorization for peer-based anomaly detection. In: ISI (2016)
40. Whiting, M., Cook, K., Paul, C., Whitley, K., Grinstein, G., Nebesh, B., Liggett, K., Cooper, M., Fallon, J.: VAST challenge 2013: Situation awareness and prospective analysis. In: VAST (2013)
41. Zhu, L., Guo, D., Yin, J., Ver Steeg, G., Galstyan, A.: Scalable temporal latent space inference for link prediction in dynamic social networks. *IEEE Trans. Knowl. Data Eng.* **28**(10), 2765–2777 (2016)